SIMULATION OF OPTICAL AND ELECTRONIC CHARACTERISTICS OF TERAHERTZ QUANTUM CASCADE LASER

MOHD ASMU'I BIN MOHD AKIL

A thesis submitted in fulfilment of the
requirements for the award of the degree of
Doctor of Philosophy (Physics)

Faculty of Science
Universiti Teknologi Malaysia

AUGUST 2021

DEDICATION

This thesis is dedicated to my father, mother, wife, sons, families and friends for their timely support during the preparation of this thesis.

ACKNOWLEDGEMENT

In the name of Allah, the Most Gracious and the Most Merciful

Alhamdulillah, all praises to Allah for the strengths and His blessing in completing this thesis. Special appreciation goes to my supervisors, Dr. Amiruddin Shaari and Prof Dr Zulkafli Othaman, for being very resourceful, constant support and great guidance. Their invaluable help of constructive comments and suggestions throughout the project and thesis works have contributed to the success of this research.

Sincere thanks express to all of my friends for their kindness and moral support during my study especially Khalid Akabli (France) for the nice code as a platform to start this research. Also, my deepest gratitude goes to my beloved family for their endless love, prayers and encouragement.

Last but not least, my further appreciation is dedicated to Ministry of High Education for providing part of the financial support through FRGS funding vot. No. R.J130000.7826.4F244. This work is impossible to finish without the financial support because it requires some tools and equipments necessary to support this research. Thank you very much.

Mohd Asmu'i, UTM Skudai

ABSTRACT

Nowadays terahertz spectroscopy is fast becoming a method of choice both in industrial and security applications. This spectroscopic method requires a device that produces broadband THz radiation. Currently one of the techniques used to generate this radiation is by using a heterogeneous AlGaAs/GaAs terahertz quantum cascade laser (THz QCL). Typically the device combines a few independent designs of active region that needs to be fabricated using very special, costly instruments and tested several times to improve its performance. A simulation model is critically needed to study the electronic transport properties of the individual designs and the optical performance of the waveguide used to support the broadband operation. Therefore the aim of this work is to establish a new model to study the electronic transport properties of four (4) experimentally established designs using the density matrix (DM) method and the optical characteristics of a narrow double metal waveguide using the finite element (FE) method. From these calculations several critical characteristics of THz QCL such as the threshold current densities, the average gain, the gain spectra, the optical mode confinement factor and the figure of merit (F.O.M) can be determined and their dependence on relevant design parameters can be studied. The results from the DM calculations show that the threshold current densities for these individual designs are in the range of 350 to 600 A cm^{-2} with the average gain of about 20 cm^{-1} and 100 cm^{-1}, without and with the stimulated emission respectively. The calculated gain spectra exhibit Lorentzian pattern over a frequency range of 1 to 5 THz. The gain spectrum of the whole system based on a combination of each individual gain spectra leads to a bandwidth of around 3 THz which is bigger than the reported bandwidth from previous experimental broadband QCL designs. Meanwhile, the result from FE method for the calculated confinement factor value obtained for the waveguide increases from 90 % to 100 % in frequency range of 2 to 4 THz. The combined effects of all the design parameters lead to a figure of merit (F.O.M) that decreases with the increase of the operating frequency. As a conclusion, a reliable prediction tool based on the DM method and FE method has been demonstrated whereby it can be used not only as a guide for broadband QCL design but also to simulate its performance before the actual design is to be fabricated.

ABSTRAK

Kini spektroskopi terahertz menjadi kaedah pilihan dalam aplikasi industri dan keselamatan. Kaedah spektroskopi ini memerlukan peranti yang menghasilkan sinaran THz berjalur lebar. Pada masa ini salah satu teknik yang digunakan untuk menghasilkan sinaran ini adalah menggunakan laser kuantum melata terahertz AlGaAs/GaAs heterogen (THz QCL). Biasanya peranti ini menggabungkan beberapa reka bentuk bebas kawasan aktif yang perlu difabrikasi menggunakan instrumen yang sangat istimewa, mahal dan diuji beberapa kali untuk meningkatkan prestasinya. Model simulasi sangat diperlukan untuk mengkaji sifat pengangkutan elektronik sesuatu reka bentuk dan prestasi optik pandu gelombang yang digunakan untuk menyokong operasi jalur lebar. Oleh yang demikian, tujuan kerja ini adalah untuk mewujudkan model baru untuk mengkaji sifat pengangkutan elektronik empat (4) reka bentuk yang dibuat secara eksperimen menggunakan kaedah matriks ketumpatan (DM) dan ciri optik pandu gelombang dua logam sempit menggunakan kaedah unsur terhingga (FE). Daripada pengiraan ini beberapa ciri kritikal THz QCL seperti ketumpatan arus ambang, gandaan purata, spektrum gandaan, faktor pengurungan mod optik dan angka merit (FOM) dapat ditentukan dan kebergantungannya pada parameter reka bentuk yang relevan dapat dikaji. Hasil daripada pengiraan DM menunjukkan bahawa ketumpatan arus ambang bagi reka bentuk individu ini adalah berada dalam julat 350 hingga 600 A cm^{-2} dengan gandaan purata kira-kira 20 cm^{-1} dan 100 cm^{-1}, masing-masing tanpa dan dengan pancaran rangsangan. Pengiraan spektrum gandaan menunjukkan corak Lorentzan dalam julat frekuensi 1 hingga 5 THz. Spektrum gandaan bagi keseluruhan sistem berdasarkan gabungan setiap spektrum gandaan individu membawa kepada lebar jalur sekitar 3 THz yang lebih besar daripada lebar jalur yang dilaporkan sebelum ini bagi reka bentuk QCL jalur lebar. Sementara itu, hasil kaedah FE untuk nilai kiraan faktor pengurungan yang diperolehi untuk pandu gelombang meningkat daripada 90 % kepada 100 % dalam julat frekuensi 2 hingga 4 THz. Kesan gabungan semua parameter reka bentuk membawa kepada angka merit (F.O.M) yang menurun dengan peningkatan frekuensi operasi. Sebagai kesimpulan, alat ramalan yang boleh dipercayai berdasarkan kaedah DM dan kaedah FE telah dapat ditunjukkan di mana ianya boleh digunakan bukan hanya sebagai panduan untuk reka bentuk QCL jalur lebar tetapi juga untuk mensimulasikan prestasinya sebelum reka bentuk sebenar dibuat.

TABLE OF CONTENTS

	TITLE	PAGE
	DECLARATION	**iii**
	DEDICATION	**iv**
	ACKNOWLEDGEMENT	**v**
	ABSTRACT	**vii**
	ABSTRAK	**viii**
	TABLE OF CONTENTS	**ix**
	LIST OF TABLES	**xii**
	LIST OF FIGURES	**xiv**
	LIST OF ABBREVIATIONS	**xviii**
	LIST OF SYMBOLS	**xx**
	LIST OF APPENDICES	**xxiv**
CHAPTER 1	**INTRODUCTION**	**1**
1.1	Introduction	1
1.2	Background of the Study	3
1.3	Statement of Problem	6
1.4	Research Objectives	7
1.5	Significance of the Study	8
1.6	Scope of Study	9
1.7	Thesis Plan	10
CHAPTER 2	**LITERATURE REVIEWS**	**13**
2.1	Introduction to Quantum Cascade Laser (QCL)	13
2.2	Simulation on Quantum Cascade Laser	17
2.3	Bandwidth of THz QCL	22
2.4	Electronic States in Heterostructures	24
2.5	Electron Scattering in Intersubband Radiative Transitions	27
	2.5.1 Introduction to Probability of Transition : Fermi's Golden Rule	28

2.5.2 Longitudional Optical (LO) Phonon Scattering 30
2.5.3 Scattering by Carriers 33
2.5.4 Interface Roughness Scattering 35
2.6 Density Matrix 37
2.7 Simulation of Terahertz Quantum Cascade Laser 39
2.8 The Gain of THz QCL 43
2.9 Waveguide of Quantum Cascade Laser 45
2.10 Dielectric Waveguides 48
2.11 Metallic Waveguide 51
2.11.1 Optical properties of metals and doped semiconductor layers 51
2.11.2 Surface plasmon 53
2.12 Simulation of Waveguides THz Quantum Cascade Lasers 56
2.13 Finite Element Method 58
2.13.1 The Rayleigh-Ritz method 60
2.13.2 The Galerkin method 63
2.13.3 FEM Process 64
2.14 FEMLAB a Partial Differential Equations Solver 66
2.14.1 Three-dimensional electromagnetic waves application mode 66
2.14.2 Two-dimensional in-plane TM waves 68
2.14.3 Two-dimensional perpendicular hybrid-mode waves 69

CHAPTER 3 RESEARCH METHODOLOGY 71
3.1 Introduction 71
3.2 Programming Flow Chart for Modelling Terahertz Quantum Cascade Laser Transports 71
3.3 Optical Modes for Broadband Double Metal Narrow Waveguides of Terahertz Quantum Cascade Laser 74
3.4 Summary of the Work 79

CHAPTER 4 RESULTS AND DISCUSSIONS 81

4.1 Introduction 81
4.2 Effects of Bias To The Envelope Wavefunctions in THz QCL 81
4.3 Results from Standard Design 84
4.4 Simulations on Other THz QCL Designs 88
4.4.1 Design (a) Dean 1 89
4.4.2 Design (b) Fathololoumi 94
4.4.3 Design (c) Belkin 97
4.4.4 Design (d) Dean 2 102
4.4.5 Summary of THz QCL Designs 105
4.5 Gain Spectra of Terahertz Quantum Cascade Laser 107
4.5.1 Design (a) Dean 1 107
4.5.2 Design (b) Fathololoumi 111
4.5.3 Design (c) Belkin 114
4.5.4 Design (d) Dean 2 117
4.5.5 Summary of Gain Spectra for THz QCLs 120
4.6 Optical Mode for Broadband Double Metal Narrow Waveguides of Terahertz Quantum Cascade Laser 121
4.6.1 Effective refractive index 126
4.6.2 Absorptive Loss of the Waveguide 127
4.6.3 Group refractive index 127
4.6.4 Confinement factor 128
4.6.5 Figure of Merit (F.O.M) 130
4.6.6 Summary of Optical Mode for Broadband Double Metal Narrow Waveguides of Terahertz Quantum Cascade Laser 131

CHAPTER 5 CONCLUSION 133
5.1 Conclusion 133
5.2 Future suggestions and recommendations 134

REFERENCES 137
LIST OF PUBLICATIONS 185

LIST OF TABLES

TABLE NO.	TITLE	PAGE
Table 2.1	Notable THz QCL Structures	15
Table 2.2	Basic parameters for GaAs and $Al_xGa_{1-x}As$.	16
Table 3.1	The $Al_{0.15}Ga_{0.85}As$/GaAs layer sequence and thicknesses (starting from the injection barrier) for RP QCLs with four different emission frequencies. Barriers are indicated in bold.	74
Table 4.1	The $Al_{0.15}Ga_{0.85}As$/GaAs layer sequence and thicknesses (starting from the injection barrier) for RP QCLs with four different emission frequencies. Barriers are indicated in bold.	89
Table 4.2	Parameters obtained from the calculation using density matrix.	107
Table 4.3	Parameters obtained from calculation of gain spectra without stimulated emission for Design (a).	110
Table 4.4	Parameters obtained from calculation of gain spectra with stimulated emission for Design (a).	110
Table 4.5	Parameters obtained from calculation of gain spectra without stimulated emission for Design (b).	114
Table 4.6	Parameters obtained from calculation of gain spectra with stimulated emission for Design (b).	114
Table 4.7	Parameters obtained from calculation of gain spectra without stimulated emission for Design (c).	117
Table 4.8	Parameters obtained from calculation of gain spectra with stimulated emission for Design (c).	117
Table 4.9	Parameters obtained from calculation of gain spectra without stimulated emission for Design (d).	120
Table 4.10	Parameters obtained from calculation of gain spectra with stimulated emission for Design (d).	120

Table 4.11	Optical modes for 30 μm ridge size at frequency 2.2, 2.4, 2.6, 2.8, 3.0, 3.2 and 3.4 THz.	122
Table 4.12	Optical modes for 40 μm ridge size at frequency 2.2, 2.4, 2.6, 2.8, 3.0, 3.2 and 3.4 THz.	123
Table B.1	Active region growth sheet of Dana Turchinkova structure.	176

LIST OF FIGURES

FIGURE NO.	TITLE	PAGE
Figure 1.1	Electromagnetic Spectrum (http://lts.fzu.cz/en/intro.htm).	1
Figure 1.2	Bandstructure of Quantum Cascade Laser.	3
Figure 2.1	(a) GaAs bandgap (300K), (b) Phonon dispersion diagram for GaAs	16
Figure 2.2	Conduction band profile and square of envelope wave functions of $Al_{0.15}Ga_{0.85}As$/GaAs layers.	25
Figure 2.3	Momentum conservation in phonon scattering.	32
Figure 2.4	Schematic representation of one period of a 4-level system under bias voltage.	40
Figure 2.5	Schematic of a symmetric dielectric waveguide.	49
Figure 2.6	Schematic of a asymmetric dielectric waveguide	50
Figure 2.7	Schematic of a dielectric-metal interface - Exponential decay of the magnetic fields.	53
Figure 2.8	Typical double metal waveguide design for THz QCL with a laser ridge along the z direction.	57
Figure 2.9	FEM example from [170]: (a) discretization of a region into triangular finite elements, (b) linear variation of trial solution within a triangular finite element.	65
Figure 3.1	Scheme of the code for the calculation of electron transport using density matrix method	72
Figure 3.2	Energies of levels 1 and 2 versus applied bias, in extended (solid lines) and localized (dashed lines) basis. The calculation of energy level anticrossing in THz QCL is the same as used by Dupont [57].	74
Figure 3.3	Double metal waveguide for broadband THz QCL	75
Figure 3.4	Scheme of the code to calculate waveguide and optical mode for THz QCL.	77

Figure 3.5	2D Terahertz QCL waveguide plot for (a) basic meshing, (b) refining the mesh and (c) plot of optical mode with the calculation of neff, overlap, f.o.m and alpha.	78
Figure 4.1	Conduction band diagram of AlGaAs/GaAs under bias (a) 4 kV/cm (c) 8 kV/cm (e) 12 kV/cm.	82
Figure 4.2	Conduction band diagram for a four level THz QCL system at 18 kV/cm operating bias for standard design.	84
Figure 4.3	Energies of levels versus electric field for THz QCL standard design.	85
Figure 4.4	The evolution of population densities by bias change without stimulated emission.	86
Figure 4.5	The evolution of population densities by bias change with stimulated emission.	87
Figure 4.6	Experimental Kumar [6] and calculated V-J curves.	88
Figure 4.7	Conduction band diagram for a four level THz QCL system at 18 kV/cm operating bias for Design (a).	90
Figure 4.8	Energies of levels versus electric field for Design (a).	91
Figure 4.9	The evolution of population densities by bias change without stimulated emission.	92
Figure 4.10	The evolution of population densities by bias change with stimulated emission.	93
Figure 4.11	The experimental and calculated V-J curve of Dean 1 design.	93
Figure 4.12	Conduction band diagram for a four level THz QCL system at 18 kV/cm operating bias for design (b).	94
Figure 4.13	Energies of levels versus electric field for design (b).	95
Figure 4.14	The evolution of population densities by bias change without stimulated emission.	96
Figure 4.15	The evolution of population densities by bias change with stimulated emission.	96
Figure 4.16	The experimental and calculated V-J curve of Fathololoumi design.	97
Figure 4.17	Conduction band diagram for a four level THz QCL system at 18 kV/cm operating bias for design (c).	98

Figure 4.18	Energies of levels versus electric field for design (c).	99
Figure 4.19	The evolution of population densities by bias change without stimulated emission.	100
Figure 4.20	The evolution of population densities by bias change with stimulated emission.	101
Figure 4.21	The experimental and calculated V-J curve of Belkin design.	101
Figure 4.22	Conduction band diagram for a four level THz QCL system at 18 kV/cm operating bias for design (d).	102
Figure 4.23	Energies of levels versus electric field for design (d).	103
Figure 4.24	The evolution of population densities by bias change without stimulated emission.	103
Figure 4.25	The evolution of population densities by bias change with stimulated emission.	104
Figure 4.26	The calculated V-J curve from the density matrix method.	105
Figure 4.27	(a) Gain spectra without the stimulated emission with the different bias voltage and (b) 3D gain spectra with contour plot.	108
Figure 4.28	(a) Gain spectra with the stimulated emission at different bias voltage and (b) 3D gain spectra with contour plot.	109
Figure 4.29	(a) Gain spectra without the stimulated emission versus the different bias voltage and (b) 3D gain spectra with contour plot.	112
Figure 4.30	(a) Gain spectra with the stimulated emission versus the different bias voltage and (b) 3D gain spectra with contour plot.	113
Figure 4.31	(a) Gain spectra without the stimulated emission with the different bias voltage and (b) 3D gain spectra with contour plot.	115
Figure 4.32	(a) Gain spectra with the stimulated emission with the different bias voltage and (b) 3D gain spectra with contour plot.	116

Figure 4.33	(a) Gain spectra without the stimulated emission with the different bias voltage and (b) 3D gain spectra with contour plot.	118
Figure 4.34	(a) Gain spectra with the stimulated emission with the different bias voltage and (b) 3D gain spectra with contour plot.	119
Figure 4.35	Optical modes of double metal waveguide at 3.1 THz : 30 μm width (a) 1^{st} (b) 2^{nd}, 40 μm width (c) 1^{st} (d) 2^{nd}.	124
Figure 4.36	1^{st} optical modes of double metal waveguides at different frequencies : 30 μm width (a) 2.1 THz (b) 3.5 THz, 40 μm width (c) 2.1 THz (d) 3.5 THz.	124
Figure 4.37	TE optical modes of double metal waveguides for 30 μm width (a) 4 THz (1^{st}) (b) 4 THz (2^{nd}) (c) 5 THz (1^{st}) (d) 5 THz (2^{nd}).	125
Figure 4.38	TE optical modes of double metal waveguides for 40 μm width (a) 4 THz (1^{st}) (b) 4 THz (2^{nd}) (c) 5 THz (1^{st}) (d) 5 THz (2^{nd}).	125
Figure 4.39	Real part of the effective refractive indices of the 1^{st} and 2^{nd} order optical modes over frequency for 30 μm and 40 μm ridge size.	127
Figure 4.40	Absorptive loss of the waveguide (α_w) over frequency for 30 μm and 40 μm ridge size.	128
Figure 4.41	Group refractive index (real) for 1^{st} and 2^{nd} order optical mode over frequency calculation for 30 μm and 40 μm ridge size.	129
Figure 4.42	Overlap or confinement factor over frequency for 30 μm and 40 μm ridge size.	129
Figure 4.43	Figure of merit value over frequency calculation for 30 μm and 40 μm ridge size.	131
Figure B.1	Courtesy of Dana Turchinkova [30].	175

LIST OF ABBREVIATIONS

THz-TDs	-	Terahertz-time domain spectroscopy
CW	-	continuous
QCL	-	Quantum Cascade Laser
GaAs	-	Gallium Arsenide
AlGaAs	-	Aluminium Gallium Arsenide
RP	-	Resonant phonon
mid-IR	-	mid-Infra Red
HQCL	-	Heterogeneous Quantum Cascade Laser
BTC	-	Bound-to-Continuum
DM	-	Density Matrix
FEM	-	Finite element method
MBE	-	molecular beam epitaxy
MOCVD	-	metal organic chemical vapour deposition
MOVPE	-	Metal Organic Vapour Phase Epitaxy
V-J	-	Voltage-Current Density
NEGF	-	Non Equilibrium Green's Function
MC	-	Monte Carlo
GaN	-	Gallium Nitride
AlGaN	-	Alluminium Gallium Nitride
ZnO	-	Zinc Oxide
MgZnO	-	Magnesium Zinc Oxide
DOS	-	density of states
LO	-	Longitudional Optical
st	-	stimulated transition
2D,3D	-	two dimensional, three dimensional
FDTD	-	finite-difference time-domain

FDM	-	Finite difference method
FWHM	-	Full Width Half Maximum
LO-phonon	-	Longitudinal Optical Phonon
MM	-	Metal-Metal
RT	-	Resonant Tunneling
RWA	-	Rotating wave approximation
SP	-	Surface Plasmon
TB	-	Tight Binding
TE	-	Transverse Electric
TMM	-	Transfer Matrix Method
TM	-	Transverse Magnetic
THz	-	Terahertz
PMC	-	Perfect magnetic conductor
PEC	-	Perfect electric conductor
BC	-	Boundary condition
PDEs	-	Partial differential equations

LIST OF SYMBOLS

f	-	frequency in GHz or THz
λ	-	Wavelength of laser [m]
J_{th}	-	Current density threshold in [A cm^{-2}]
Γ	-	Confinement factor
m_e	-	Effective electron mass
Å	-	Angstrom (10^{-10} m)
$U_{n,0}(r)$	-	Bloch state wavefunction at the band minimum
$F(r)$	-	envelope function
$m^*(z)$	-	spatially varying effective mass
$E_c(z)$	-	potential represents the conduction band diagram
$\nabla_{\parallel}$	-	in-plane differential operator
k_{xy}	-	in-plane wavevector
S	-	normalization area
$E_c(z)$	-	conduction band profile
$\Phi(z)$	-	electrostatic potential
$\epsilon(z)$	-	spatially varying permittivity
$\rho(z)$	-	charge density
$\hat{W}(t)$	-	observable of a perturbation
$P_{if}(t)$	-	probability of finding the system in another state at time t
$W_{nk}(t)$	-	matrix element
b_n	-	constant dependent on the initial conditions
ω_{nk}	-	the Bohr frequency
$\rho(E_f)$	-	density of states
ω_{if}	-	phenomenon of resonance
H'_{LO}	-	the perturbation
K_{xy}	-	wave vector of the phonon

$\hbar\omega, E$	-	energy
$\epsilon, \epsilon_\infty, \epsilon_s$	-	permittivity of the material
H_{e-e}	-	Coulomb interaction
Δ	-	Gaussian distribution of height
a_n	-	complex amplitude or coefficient of the n^{th} state at time t
$\hat{O}$	-	an observable (self-adjoint operator)
$\hat{\rho}(t)$	-	density operator for a system in state $\|\psi(t)\rangle$
Ω_{ij}	-	coupling strength between two level i j
τ_{ij}	-	time of relaxation i j
$\Delta\rho = \rho_{22} - \rho_{33}$	-	population inversion
Tr	-	trace operation of a matrix
$\hat{v}$	-	velocity operator
$\hat{\rho}$	-	density operator
$\hat{z}$	-	position operator
$\mathcal{P}(t)$	-	electrical polarization
V_{ac}	-	volume of the active region
$\chi(\omega)$	-	induced electrical susceptibility
$g(\omega)$	-	optical gain coefficient (per meter)
$\chi''(\omega)$	-	susceptibility
n_r	-	refractive index of the medium
$\vec{\mathcal{E}}$	-	electric fields
$\vec{H}$	-	magnetic fields
$\vec{D}$	-	electric displacement
$\vec{B}$	-	magnetic induction
μ	-	permeability of the medium
$\mathcal{E}_\perp$	-	perpendicular of electric field
$\mathcal{E}_\parallel$	-	parallel of electric field
$H_\perp$	-	perpendicular of magnetic field

$H_{\parallel}$	-	parallel of magnetic field
A	-	complex eigenvalue
δ	-	damping of the solution
δ_z	-	damping in the propagation direction
n	-	refractive index
ω_p	-	plasma angular frequency
α	-	attenuation constant using the Beer law
β	-	propagation constant
σ	-	electrical conductivity
$\hbar$	-	Reduced Planck constant 1.05×10^{-34} [J.s]
e	-	Elementary charge 1.60×10^{-19} [C]
k_B	-	Boltzmann constant 1.38×10^{-23} [J/K]
m_e	-	Rest mass of free electron 9.11×10^{-31} [kg]
E_k	-	Kinetic energy
k	-	Wavevector
m	-	Mass
t	-	Time
ψ, ϕ	-	Wavefunction
ω	-	Angular frequency
E_{LO}	-	Energy of longitudinal optical phonon
ρ_{ij}	-	Elements of density matrix
c	-	Speed of light in vacuum 3.00×10^8 [m/s]
Γ	-	Overlap factor between the optical mode and active region
σ	-	Cross section per unit time $[m^2/s]$
d_{ij}	-	Matrix element of $\lvert z \rvert$ [m]
$\lvert e \rvert d_{ij}$	-	Element of electric dipole matrix [C.m]
n	-	Refractive index of the medium
S	-	Surface density of photons $[1/m^2]$

q	-	Charge of electron [C]
ε_0	-	Vacuum permittivity 8.8541×10^{-12} [A.s/V.m]
L_p	-	Length of period [m]
γ_{23}	-	FWHM of the spontaneous emission line [s]
$2\hbar\Omega$	-	Coupling energy
J	-	Current density [A/m^2]
I	-	Current [A]
g	-	Optical gain [m^{-1}]

LIST OF APPENDICES

APPENDIX	TITLE	PAGE
Appendix A	The Code of QCL	155
Appendix B	Heterogeneous THz QCL Waveguide	175

CHAPTER 1

INTRODUCTION

1.1 Introduction

Terahertz (THz) region of the electromagnetic spectrum (frequency f ~ 300 GHz – 10 THz; wavelength λ ~1000 – 30 μm; energy ~ 1 – 40 meV) opens up a new triumph in spectroscopy and imaging field because of its abilities or behaviors which are different from other electromagnetic sources. THz radiation located between the microwave and far-infrared regions in electromagnetic spectrum (Figure 1.1). Historically it is the least explored region and the last to be discovered because there is a gap between the electronic transitions (microwave) and optical transitions, making it difficult to develop suitable and reliable radiation sources. Terahertz is virtually unused portion of light spectrum nestled between photonics and electronics. It can "see" more color than humans can as they reflect different colors of light in various patterns, textures and signatures. Terahertz radiation is safe because it is a non-ionizing form of electromagnetic radiation and can penetrate many solids but not to water or metals.

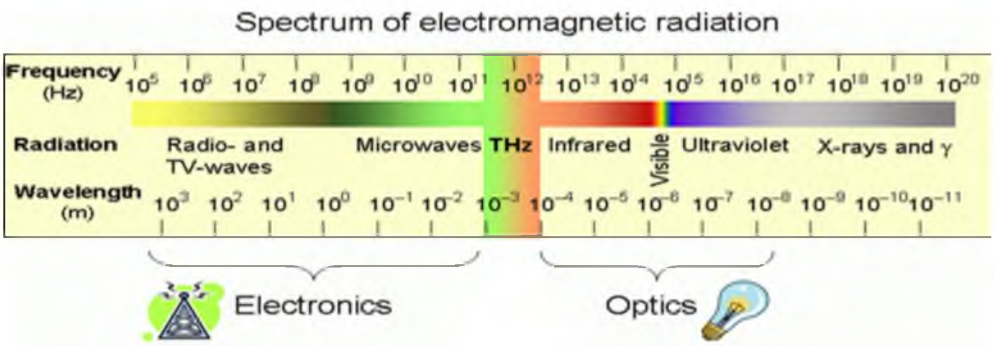

Figure 1.1 Electromagnetic Spectrum (http://lts.fzu.cz/en/intro.htm).

These characteristics make it very suitable to be used in many applications such as security, medical and biological imaging, communications and quality assurance. Currently, there are many types of commercially available THz generation techniques such as gas laser, time domain technique (THz-TDS), heterodyne technique, quantum cascade laser (QCL) and others to name a few [1]. One of the significant source is a THz quantum cascade laser (QCL) which is the subject of this research work. This semiconductor device (THz QCL) have been reported to generate monochromatic, coherent, high and stable optical power THz radiation within a reduced compact package [2, 3, 4]. Also, it can be operated in both pulse and CW (continuous) mode operations.

THz QCL is a unipolar solid state device, consisting of a layered semiconductor superlattice structure. The operation of THz QCL is based on the processes whereby electrons are injected into the structure and transported (cascaded) through a series of repeated injector-active regions emitting photons as they pass through each active region. Figure 1.2 shown typical bandstructure of QCL structure. In this figure the square like shape is a superlattice of barrier and well sandwich one to the others. In this research, the barrier is AlGaAs and the well is GaAs. Furthermore the wave shape is a envelope wavefunction of the energy state in the well. The envelope wavefunction show the probability density of the electron consists in the state.

Until now, many laboratories are reported to grow superlattice structures for the QCLs using compounds from chemical elements in the III-V group, namely the GaAs, InAs, InP based superlattice, and from elements of group IV such as the Si based superlattice. Also, there are several widely used THz QCL designs such as the bound-to-continuum, the chirped superlattice and resonant phonon [5]. Each THz QCL design has its own mechanism of operation. The infamous THz QCL design because of the temperature and lasing output that become a standard is based on resonant phonon (RP) design was publish by Kumar *et al.* [6]. The THz radiation produced by THz QCL device can be engineered by designing the behaviour of an electron transport inside the active regions. It can be done through a change of the barrier height and layer thickness (width) to produce population inversion and laser emission at certain wavelength. This

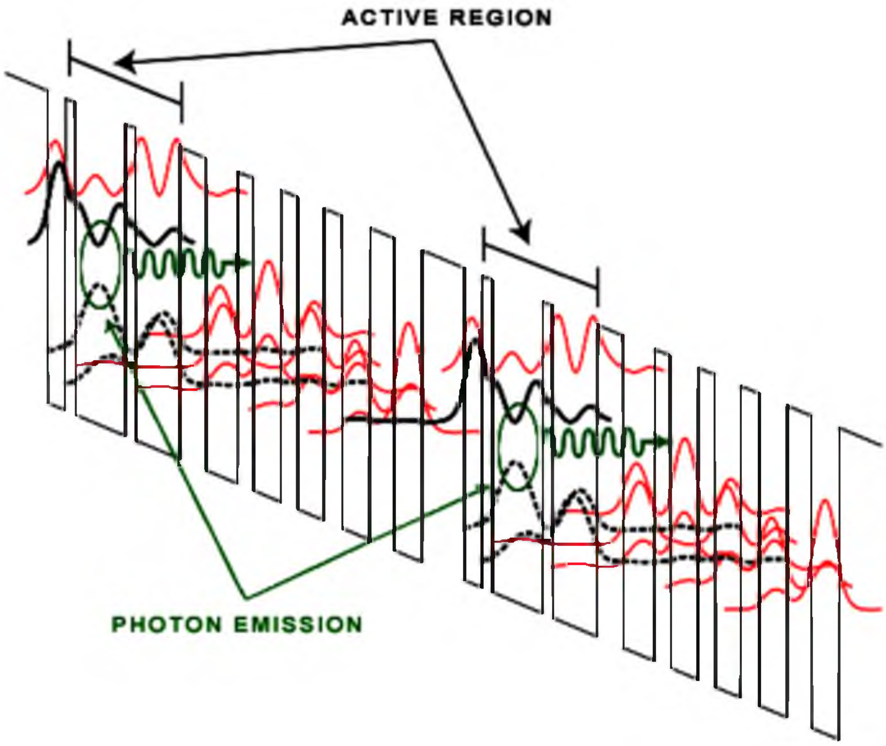

Figure 1.2   Bandstructure of Quantum Cascade Laser.

is why the frequency or wavelength of generated radiation can be tuned by injection of electrons and bias applied to the device.

1.2 Background of the Study

Over the past decade there has been significant development of THz QCL-based spectroscopy and imaging systems, driven by the opportunities presented by the unique properties of THz radiation. Unlike millimetre-waves, THz radiation excites vibrational modes in many organic and inorganic materials, enabling samples to be discriminated chemically as well as providing sensitivity to differences in crystalline structure [7, 8, 9]. The THz radiation is non-ionizing and able to penetrate dry non-polar materials such as paper and plastic packaging providing significant advantages in investigation of concealed samples. These properties make THz radiation particularly suitable for a wide range of applications including non-destructive inspection, security screening, and biomedicine, as well as atmospheric science and astronomy [10, 1]. Examples of THz QCL-based systems include compact imaging and displacement sensing schemes utilizing the self-mixing effect in QCLs [11, 12], diffuse reflection [13, 14] and transmission imaging systems for spectroscopic sample analysis [15], imaging systems for biomedical applications [16] and non-destructive evaluation [17], as well as heterodyne mixing schemes [18, 19] for applications including high-resolution gas spectroscopy [20].

Although THz QCL has the ability to produce high optical power and to tune the wavelength it produces, some specialized applications such as tomography critically need source with broadband emission. In such applications, the need for a source with a broad range of optical emissions becomes crucial especially for studying the absorption of the THz radiation by certain materials in the form of solid, liquid, gas or plasma [21, 22, 11, 23, 24, 15]. The fundamental mechanism behind the laser action leads, in general, only to a narrowband or single-wavelength emission. Several approaches for achieving spectrally broadband laser action have been put forward, such as enhancing the optical feedback in the wings of the gain spectrum [25, 26], multi-peaked gain spectra [27], and the most favourable technique at present, the ultrashort pulse excitation [28, 29]. Each of these approaches has a drawback, such as a complex external laser cavity configuration, a non-flat optical gain envelope function, and inability to operate in continuous mode respectively.

Common QCLs are homogeneous which means that the active region of the QCL is embedded in the optical waveguide and composed of a repetition of periods based on a single active region structure or design. These homogeneous QCLs are characterized by homogeneous line-width broadening which means that the system suffers from gain narrowing due to mode-competition and the envelope of the emitted spectrum is modulated by a Lorentzian function. Hence, in order to obtain a flat gain medium, a simple design optimization is not enough [30].

This issue has been introduced by Gmachl et al., [31] for mid-IR QCL where a number of dissimilar intersubband optical transitions are made to cooperate in order to give a broadband optical emission from 5 to 8 μm wavelength. The same concept has also been used by Turcinkova *et al.*, [30] to have a laser system that consists of many independent segments whose transition line shapes are designed separately. The final gain spectrum of such a system would be the sum of the contributing transitions. This is achieved by stacking different active-region designs into a common waveguide, obtaining a so-called heterogeneous QCL (HQCL). Although, the concept to improve gain by using HQCL has been extensively studied in the mid-infrared range but it has not been fully developed in the far infra-red or THz region.

Equally critical, the performance of laser is also strongly dependent on the waveguide design. In QCL there are commonly two types of waveguides namely the surface plasmon waveguide and double metal waveguide. Double metal waveguide is well known to support broadband emission [32, 33]. Previous studies on THz QCL using double metal waveguide have been done experimentally by Kumar et. al. [34] and Fathololoumi [35]. Both studies focus on the performance of THz QCLs at high temperature but these lasers do not produce broadband emission. Currently, no experimental work on the device is able to cover the spectral range from 1 to 4 THz simultaneously. The widest spectral coverage has been demonstrated and achieved by Rösch *et al.* (2014) [36]. This device employs four active region segments or called designs to produce optical emission from 1.64 to 3.35 THz. The detailed study on optical waveguide for broadband THz QCL is still therefore insufficient compared to that of the broadband mid-IR QCL [31, 37, 38, 39].

Even though double metal waveguides can support broadband emission, but future applications especially in THz spectroscopy and imaging require devices to become more compact with narrow waveguides. Thus a new design with a trade-off between the capability to support the required optical modes and to operate without exceeding losses is needed. The common width of a THz QCL waveguide is usually more than 100 µm [40]. A narrow waveguide is suspected to be more advantages to the performance of a THz QCL due to the fact that it requires less injection current to start lasing. Furthermore it also makes the THz QCL more compact and portable for on-site spectroscopy [41].

1.3 Statement of Problem

The important of the broadband THz mainly used as an amplifier in THz TDS systems, as the gain medium in a tunable cavity or in modelocking [42] and astrophysics/atmospheric sensing as explained in Dana Turchinkova thesis [43] to name a few. Despite the abilities of broadband THz QCL as mentioned before, the growth, processing and testing of the device is an expensive processes. Furthermore, the basic principle of the performances to design a broadband THz QCL is still lacking, even though some experimental studies on a broad range of THz QCLs have been conducted by [44, 45, 46, 36, 30]. The bandwidth of the upstanding work is 1.71 THz [36] produce optical emission from 1.64 to 3.35 THz surpass the work of [30] that produce bandwidth 1 THz (laser emission from 2.2 to 3.2 THz). Both of this researcher used the same QCL design as shown in Appendix C. This is due to the drawback of experimental studies where the manipulation of microscopic mechanism is limited such as the the efficiency of injection and extraction to the device and the population density of the laser state that eventually lead to the voltage-current density (V-J) and gain spectra. The lacking in understanding of this basic principle before doing an experiment will lead to the inefficient research. In addition, most of the experimental works for broadband THz use the bound-to-continuum (BTC) design. Although usually the spectrum of BTC is rather broad compared to the resonant phonon design, but the resonant phonon gives the highest optical performance. This is due to the advantages of resonant phonon design which it has a higher operating temperature and can achieve higher optical power usually over 100 mW [5].

To overcome the issue, the need of computational studies on the performance of the broadband resonant phonon THz QCL is highly demanding on the development of THz HQCL field or known as broadband THz QCL. This is due to the importance of minimizing the cost of the fabrication and testing of the unoperated devices. The strategy is to calculate the performance that can generate and support the broadband emission for this THz QCL. The generation of broadband emission can be understood by the study of electronic transport mechanism in the four active regions used in broadband THz QCL. The density matrix method was chosen because its can handle a mix quantum states to model QCL. Other methods such as the non equilibrium Green's function, for example, is known capable to study full quantum system but it is rather too complicated and time consuming to calculate the problem.

For studying the waveguide whether or not it can support the broadband emission, the finite element method (FEM) calculation was used to study the optical modes of the waveguide. This well known technique is essential to establish the initial broadband profile of the broadband THz QCL.

1.4 Research Objectives

The aim of this research is to study the parameters involved in the performance of broadband THz QCL. The codes obtained from Laboratoire Materiaux et Phenomenes Quantiques, Universite Paris Diderot VII by personal communication are used as a starting point of this research. One of the original code calculates envelope function to study the bandstructure of a QCL only. The improvements have been made to include parameters necessary to calculate the electron transport such as improving the density matrix model itself for the purpose to study the performance of the device. Also, addition has been made to the code making it capable to do a full automation to calculate parameters such as couplings of the state, population density of the state and current density over the range of bias. Lastly, the gain over frequency relation is added to make the studies of broadband THz QCL feasible. Another code is the finite element method (FEM) code to solve electromagnetic problem. This can be done by achieving the following objectives:

- To improve the code obtained from Laboratoire Materiaux et Phenomenes Quantiques, Universite Paris Diderot VII from calculation of bandstructure only to calculation of density matrix to solve transport in THzQCL resonant phonon design. The calculation of time of relaxation and density of state every level are coded. Plotting coupling of state, population density and current density of the THz QCL structure. Four different active regions from experimental designs by Dean 1 and 2 [47], Fathololoumi [48] and Belkin [49] will be used as a template for study the broadband THz QCL.

- To incorporated rotating wave approximation model to density matrix for calculation of gain spectra target from 1 to 5 THz region. The validation of the modified code was implemented by running the four different active regions above to obtained gain spectrum of the active regions. This is an indication of responsive of the active regions to produce optical spectrum in the region it produce.
- To calculate full optical spectrum of the active region structure with different bias. Because every electrical bias the characteristics of optical spectrum different. This is depend on the alignment of state inside the active region. Obtained a 3D graph of bias-gain-frequency.
- To compute using matlab program to study optical mode of the THz QCL narrow waveguide. The optical mode characteristics is important to observed the behaviour of each waveguide with narrow waveguide design and metal-metal waveguide for range of THz region 1 to 5 THz. Obtaining the result of 2D optical mode distribution at the facet of laser and plotting other parameter such as effective refractive index, absorption loss, group refractive index, confinement factor and figure of merit.

1.5 Significance of the Study

The motivation of this research is to figure out the mechanisms contributing to the broadband emission of QCL. By understanding the transport properties inside this device one is able to fundamentally manipulate or engineer the bandstructure to systematically improve its optical gain. This will lead to capability that gives a broadband THz emission and eventually opens up new applications in THz spectroscopy. The demanding applications in THz spectroscopy need a stable optical source that can achieve a super-continuum for THz radiation. A super-continuum is a phenomenon where the power over a broad frequency range is almost constant. This capability is very useful for simultaneous scanning over broad frequency of the sample rather than taking time to tune over a wide range of frequency.

Also, the aim for this research is to help lowering the production cost of broadband THz QCL because the techniques to grow such a nano structure device are limited to molecular beam epitaxy (MBE) [50] and metal organic chemical vapour deposition (MOCVD) [51, 52, 53]. These techniques are very costly and normally lead to trial-and-error production processes. The production of QCL will become more efficient in term of time and financial by incorporating theoretical and simulation work to predict the performance of the device in advance. Furthermore, the designer can improve the output performance of the device to meet the application needed for customer demand.

1.6 Scope of Study

The work on this research emphasize on the simulation of electrical and optical performance of the resonant phonon THz QCL to achieve a broad range emission between 1 to 5 THz. Resonant phonon design is chosen rather than bound-to-continuum design because of its excellent performances in producing the highest single THz emission, even though the bound-to-continuum produces more broad emission than resonant phonon. This THz QCL consists of combination of four individual active regions and double metal waveguide to produce broad range emission. The materials of this THz QCL are based on established compound semiconductors namely $Al_{0.15}Ga_{0.85}As$ and GaAs.

The developed codes were compiled using Gnu C Compiler or GCC version 4.2.2 in Ubuntu 14.12 linux distribution. In this work, the electrical and optical performances are achieved through the calculation of voltage-current density (V-J) characteristics and gain spectrum profile respectively. In this calculation the effect of temperature is neglected and the temperature is assumed to be in cryogenic temperature of 4 Kelvin.

Furthermore, this work also focuses on the study of THz QCL waveguide. The double metal waveguide is chosen to support the broadband frequency of the THz emission produced by the active regions of this study. The optical mode characteristic of this waveguide is calculated using finite element method (FEM). In this calculation, the calculation of the mode is based on 2D mode calculation with neglecting the resonator effect of laser ridge. The optical mode that have been studied through the parameters such as the effective refractive index, losses of optical mode, the overlap of the mode, group refractive index and figure of merit.

1.7 Thesis Plan

This thesis comprises five chapters. The first chapter discusses the introduction to THz QCL and its basic operations as well as the needs for broadband THz QCL and the problems faced to achieve the best design. This will be solved by developing an electronic transport calculation for THz QCL. The objectives for this study will also be explained along with the scope of the research and the potential applications.

The second chapter deals with the literature review on the previous studies done by researchers all over the world on experimental performance of the device and theoretical efforts to improve the device performance. This chapter will briefly describe the basics of THz QCL including its operations and continue to discuss heterogeneous QCL and its operations. The transport and scattering inside of the THz QCL will also be discussed here. The chapter will focus on theoretical calculation to solve the transport of THz QCL using density matrix method. Also, a basic theory on electromagnetic of transmission line with the focus on waveguide for QCL device. At the end of the chapter some basic theory on terahertz QCL will be discussed.

The third chapter describes the methodology adopted in this research. Initially the chapter starts with the development of a quantum system by using density matrix method (DMM). The theoretical framework is utilized to 4-level QCL system and compared to experimental structure. Next, further improvement on the method to establish the density matrix method to solve 4-level system is discussed. The DMM is considered excellent when it can explain the performance and electronic transport of the existing single design THz QCL. Parameters describing the performance of the device are the voltage-current density (V-J) and gain. Detail explanation on transport parameters such as the population density of the level and the time of relaxation will also be discussed. Also the waveguide of THz QCL will be discussed in the methodology and focused on the flow chart of the optical mode calculations. This will give the insight on the optical mode related parameters such as waveguide loss, confinement factor, effective refractive index and figure of merit.

The fourth chapter deals with the analysis on the results of each process explained in chapter three. The analysis is done to improve the theoretical formalism of the density matrix method and also to improve the transport parameters by identifying certain physical parameters on the device. The outputs of these processes are used to predict the performance, study the transport and improve the design of broadband THz QCL. Finally, the result on optical waveguide and mode are used to design a suitable waveguide for broadband THz QCL. Without the calculation of optical waveguide, the laser will not be able to produce a broadband emission because the optical mode will be dispersed even though the active region is designed to achieve broadband emission.

The final chapter summarizes the findings and comments on results and findings of the research work to develop calculation tools to analyse and explain the electronic transport in broadband THz QCL or known as heterogeneous THz QCL. A recommendation is also given at the end of this thesis for potential further study.

REFERENCES

1. Tonouchi, M. Cutting-edge terahertz technology. *Nature Photonics*, 2007. 1: 97–105.

2. Faist, J., Capasso, F., Sivco, D., Sirtori, C., Hutchinson, A. and Cho, A. Quantum Cascade Laser. *Science*, 1994. 264(5158): 553–556.

3. Köhler, R., Tredicucci, A., Beltram, F., Beere, H. E., Linfield, E. H., Davies, A. G., Ritchie, D. A., Iotti, R. C. and Rossi, F. Terahertz semiconductor-heterostructure laser. *Nature*, 2002. 417: 156–159.

4. Kohler, R., Tredicucci, a., Beltram, F., Beere, H., Linfield, E., Davies, G., Ritchie, D., Iotti, R. and Rossi, F. Terahertz semiconductor heterostructure laser. *Physics of Semiconductors 2002, Proceedings*, 2003. 171: 145–152.

5. Williams, B. S. Terahertz quantum-cascade lasers. *Nature Photonics*, 2007. 1: 517–525.

6. Kumar, S., Hu, Q. and Reno, J. L. 186 K operation of terahertz quantum-cascade lasers based on a diagonal design. *Applied Physics Letters*, 2009. 94.

7. Davies, A. G., Burnett, A. D., Fan, W., Linfield, E. H. and Cunningham, J. E. Terahertz spectroscopy of explosives and drugs. *Materials Today*, 2008. 11(3): 18–26.

8. Zeitler, J. A., Taday, P. F., Newnham, D. a., Pepper, M., Gordon, K. C. and Rades, T. Terahertz pulsed spectroscopy and imaging in the pharmaceutical setting–a review. *The Journal of pharmacy and pharmacology*, 2007. 59(2): 209–223.

9. Shen, Y. C. Terahertz pulsed spectroscopy and imaging for pharmaceutical applications: A review. *International Journal of Pharmaceutics*, 2011. 417(1-2): 48–60.

10. Mittleman, D. *Sensing with Terahertz Radiation*. Springer Series in Optical Sciences. Berlin: Springer. 2003.

11. Dean, P., Lim, Y. L., Valavanis, A., Kliese, R., Nikolić, M., Khanna, S. P., Lachab, M., Indjin, D., Ikonić, Z., Harrison, P., Rakić, A. D., Linfield, E. H. and Davies, A. G. Terahertz imaging through self-mixing in a quantum cascade laser. *Optics letters*, 2011. 36(13): 2587–2589.

12. Leng Lim, Y., Dean, P., NikolicÌĄ, M., Kliese, R., Khanna, S. P., Lachab, M., Valavanis, A., Indjin, D., IkonicÌĄ, Z., Harrison, P., Linfield, E. H., Giles Davies, A., Wilson, S. J. and RakicÌĄ, A. D. Demonstration of a self-mixing displacement sensor based on terahertz quantum cascade lasers. *Applied Physics Letters*, 2011. 99(8): 081108.

13. Dean, P., Shaukat, M. U., Khanna, S. P., Chakraborty, S., Lachab, M., Burnett, A., Davies, G. and Linfield, E. H. Absorption-sensitive diffuse reflection imaging of concealed powders using a terahertz quantum cascade laser. *Optics express*, 2008. 16(9): 5997–6007.

14. Dean, P., Burnett, A. D., Tych, K., Khanna, S. P., Lachab, M., Cunningham, J. E., Linfield, E. H. and Davies, A. G. Measurement and analysis of the diffuse reflectance of powdered samples at terahertz frequencies using a quantum cascade laser. *The Journal of chemical physics*, 2011. 134(13): 134304.

15. Dean, P., Saat, N. K., Khanna, S. P., Salih, M., Burnett, A., Cunningham, J., Linfield, E. H. and Davies, A. G. Dual-frequency imaging using an electrically tunable terahertz quantum cascade laser. *Optics express*, 2009. 17: 20631–20641.

16. Kim, S. M., Hatami, F., Harris, J. S., Kurian, A. W., Ford, J., King, D., Scalari, G., Giovannini, M., Hoyler, N., Faist, J. and Harris, G. Biomedical terahertz imaging with a quantum cascade laser. *Applied Physics Letters*, 2006. 88(15).

17. Kumar, S. and Lee, A. W. M. Resonant-phonon terahertz quantum-cascade lasers and video-rate terahertz imaging. *IEEE Journal on Selected Topics in Quantum Electronics*, 2008. 14(2): 333–344.

18. Khosropanah, P., Zhang, W., Hovenier, J. N., Gao, J. R., Klapwijk, T. M., Amanti, M. I., Scalari, G. and Faist, J. 3.4 THz heterodyne receiver using a hot electron bolometer and a distributed feedback quantum cascade laser. *Journal of Applied Physics*, 2008. 104(11).

19. Hajenius, M., Khosropanah, P., Hovenier, J. N., Gao, J. R., Klapwijk, T. M., Barbieri, S., Dhillon, S., Filloux, P., Sirtori, C., Ritchie, D. A. and Beere, H. E. Surface plasmon quantum cascade lasers as terahertz local oscillators. *Optics letters*, 2008. 33: 312–314.

20. HüÌĹbers, H. W., Pavlov, S. G., Richter, H., Semenov, A. D., Mahler, L., Tredicucci, A., Beere, H. E. and Ritchie, D. A. High-resolution gas phase spectroscopy with a distributed feedback terahertz quantum cascade laser. *Applied Physics Letters*, 2006. 89(6): 061115.

21. Darmo, J., Tamosiunas, V., Fasching, G., Kröll, J., Unterrainer, K., Beck, M., Giovannini, M., Faist, J., Kremser, C. and Debbage, P. Imaging with a Terahertz quantum cascade laser. *Optics express*, 2004. 12: 1879–1884.

22. Nguyen, K. L., Johns, M. L., Gladden, L., Worrall, C. H., Alexander, P., Beere, H. E., Pepper, M., Ritchie, D. A., Alton, J., Barbieri, S. and Linfield, E. H. Three-dimensional imaging with a terahertz quantum cascade laser. *Optics express*, 2006. 14: 2123–2129.

23. Dean, P., Valavanis, A., Keeley, J., Bertling, K., Lim, Y. L., Alhathlool, R., Burnett, a. D., Li, L. H., Khanna, S. P., Indjin, D., Taimre, T., Rakić, a. D., Linfield, E. H. and Davies, a. G. Terahertz imaging using quantum cascade lasersâĂŤa review of systems and applications. *Journal of Physics D: Applied Physics*, 2014. 47(37): 374008.

24. Jepsen, P. U., Cooke, D. G. and Koch, M. Terahertz spectroscopy and imaging âĂŞ Modern techniques and applications. *Laser & Photonics Reviews*, 2011. 5(1): 124–166.

25. Mittlelstein, M. Broadband tenability of gain-flattened quantum well semiconductor lasers with external grating. *Appl. Phys. Lett.*, 1989. 54: 1092–1094.

26. Hall, D. C. Broadband long-wavelength operation (9700 Å $\geq \lambda \geq$ 8700 Å) of AlGaAs-GaAs-InGaAs quantum well heterostructure lasers in an external grating cavity. *Appl. Phys. Lett.*, 1989. 55: 752–754.

27. Chernikov, S. V., Zhu, Y., Taylor, J. R. and Gapontsev, V. P. Supercontinuum self-Q-switched ytterbium fiber laser. *Optics letters*, 1997. 22: 298–300.

28. Spielmann, C., Curley, P. F., Brabec, T. and Krausz, F. Ultrabroadband femtosecond lasers. *IEEE Journal of Quantum Electronics*, 1994. 30: 1100–1114.

29. Ranka, J. K., Windeler, R. S. and Stentz, A. J. Visible continuum generation in air-silica microstructure optical fibers with anomalous dispersion at 800 nm. *Optics letters*, 2000. 25: 25–27.

30. Turčinková, D., Scalari, G., Castellano, F., Amanti, M. I., Beck, M. and Faist, J. Ultra-broadband heterogeneous quantum cascade laser emitting from 2.2 to 3.2 THz. *Applied Physics Letters*, 2011. 99.

31. Gmachl, C., Sivco, D. L., Colombelli, R., Capasso, F. and Cho, A. Y. Ultra-broadband semiconductor laser. *Nature*, 2002. 415: 883–887.

32. Fan, J. a., Belkin, M. a., Capasso, F., Khanna, S., Lachab, M., Davies, a. G. and Linfield, E. H. Surface emitting terahertz quantum cascade laser with a double-metal waveguide. *Optics express*, 2006. 14(24): 11672–80.

33. Fan, W. H., Burnett, A., Upadhya, P. C., Cunningham, J., Linfield, E. H. and Davies, A. G. Far-infrared spectroscopic characterization of explosives for security applications using broadband terahertz time-domain spectroscopy. *Applied spectroscopy*, 2007. 61(6): 638–43.

34. Kumar, S., Williams, B. S., Qin, Q., Lee, A. W., Hu, Q. and Reno, J. L. Surface-emitting distributed feedback terahertz quantum-cascade lasers in metal-metal waveguides. *Optics express*, 2007. 15: 113–128.

35. Fathololoumi, S., Dupont, E., Razavipour, S. G., Laframboise, S. R., Delage, A., Wasilewski, Z. R., Bezinger, A., Rafi, G. Z., Safavi-Naeini, S., Ban, D. and Liu, H. C. Electrically switching transverse modes in high power THz quantum cascade lasers. *Optics express*, 2010. 18: 10036–10048.

36. Rösch, M., Scalari, G., Beck, M. and Faist, J. Octave-spanning semiconductor laser. *Nature Photonics*, 2014. 9(1): 42–47.

37. Hugi, A., Terazzi, R., Bonetti, Y., Wittmann, A., Fischer, M., Beck, M., Faist, J. and Gini, E. External cavity quantum cascade laser tunable from 7.6 to 11.4 μm. *Applied Physics Letters*, 2009. 95.

38. Freeman, J. R., Marshall, O. P., Beere, H. E. and Ritchie, D. A. Electrically switchable emission in terahertz quantum cascade lasers. *Optics express*, 2008. 16: 19830–19835.

39. Freeman, J. R., Madeo, J., Brewer, A., Dhillon, S., Marshall, O. P., Jukam, N., Oustinov, D., Tignon, J., Beere, H. E. and Ritchie, D. A. Dual wavelength emission from a terahertz quantum cascade laser. *Applied Physics Letters*, 2010. 96(2010): 51120.

40. Fathololoumi, S., Dupont, E., Razavipour, S. G., Laframboise, S. R., Parent, G., Wasilewski, Z., Liu, H. C. and Ban, D. On metal contacts of terahertz quantum cascade lasers with a metal–metal waveguide. *Semiconductor Science and Technology*, 2011. 26(10): 105021.

41. Bacon, D. R., Freeman, J. R., Mohandas, R. A., Li, L., Linfield, E. H., Davies, A. G. and Dean, P. Gain recovery time in a terahertz quantum cascade laser. *Applied Physics Letters*, 2016. 108(8): 081104.

42. Freeman, J. R., Brewer, A., MadÃĺo, J., CavaliÃĺ, P., Dhillon, S. S., Tignon, J., Beere, H. E. and Ritchie, D. A. Heterogeneous THz quantum cascade lasers: Broadband operation. *2011 International Conference on Infrared, Millimeter, and Terahertz Waves*. 2011. 1–2.

43. Turcinkova, D. *Terahertz Quantum Cascade Lasers for Astronomical Applications*. Ph.D. Thesis. Eth Zurich. 2014.

44. Fujita, K., Hitaka, M., Ito, A., Yamanishi, M., Dougakiuchi, T. and Edamura, T. Ultra-broadband room-temperature terahertz quantum cascade laser sources based on difference frequency generation. *Optics Express*, 2016. 24(15): 16357–16365.

45. Li, L. H., Garrasi, K., Kundu, I., Han, Y. J., Salih, M., Vitiello, M. S., Davies, A. G. and Linfield, E. H. Broadband heterogeneous terahertz frequency quantum cascade laser. *Electronics Letters*, 2018. 54(21): 1229–1231.

46. Demtl, C. G., Scalari, G., Beck, M., Faist, J., Unterraincr, K. and Darmo, J. Gain recovery dynamics in broadband terahertz quantum cascade lasers. *2018 43rd International Conference on Infrared, Millimeter, and Terahertz Waves (IRMMW-THz)*. 2018. 1–2.

47. Dean, P., Salih, M., Khanna, S. P., Li, L. H., Saat, N. K., Valavanis, A., Burnett, A., Cunningham, J. E., Davies, a. G. and Linfield, E. H. Resonant-phonon depopulation terahertz quantum cascade lasers and their application in spectroscopic imaging. *Semiconductor Science and Technology*, 2012. 27(9): 094004.

48. Fathololoumi, S., Dupont, E., Chan, C., Wasilewski, Z., Laframboise, S., Ban, D., Mátyás, A., Jirauschek, C., Hu, Q. and Liu, H. C. Terahertz quantum cascade lasers operating up to ~ 200 K with optimized oscillator strength and improved injection tunneling. *Optics Express*, 2012. 20: 3866.

49. Belkin, M. A., Qi Jie, W., Pflugl, C., Belyanin, A., Khanna, S. P., Davies, A. G., Linfield, E. H. and Capasso, F. High-Temperature Operation of Terahertz Quantum Cascade Laser Sources. *Selected Topics in Quantum Electronics, IEEE Journal of*, 2009. 15(3): 952–967.

50. Schrenk, W., Pflugl, C., Austerer, M., Golka, S., Strasser, G., Green, R., Wilson, L., Revin, D., Zibik, E., Cockburn, J., Tey, C., Krysa, A., Roberts, J. and Cullis, A. Surface emission from MBE and MOVPE grown quantum cascade lasers. *(CLEO). Conference on Lasers and Electro-Optics, 2005.*, 2005. 1.

51. Krysa, A., Roberts, J., Green, R., Wilson, L., Page, H., Garcia, M. and Cockburn, J. MOVPE-grown quantum cascade lasers operating at âĹij9μm wavelength. *Journal of Crystal Growth*, 2004. 272: 682–685.

52. Wilson, W., Green, R., Revin, D., Cockburn, J., Krysa, A. and Roberts, J. High performance MOVPE grown quantum cascade lasers. *Conference on Lasers and Electro-Optics, 2004. (CLEO).*, 2004. 1.

53. Liu, Z., Wasserman, D., Howard, S. S., Hoffman, A. J., Gmachl, C. F., Wang, X., Tanbun-Ek, T., Cheng, L. and Choa, F. S. Room-temperature continuous-wave quantum cascade lasers grown by MOCVD without lateral regrowth. *IEEE Photonics Technology Letters*, 2006. 18: 1347–1349.

54. Kazarinov, R. F. and Suris, R. A. Possibility of the amplification of electromagnetic waves in a semiconductor with a superlattice. *Soviet Physics - Semiconductors*, 1971. 5: 707–709.

55. Ajili, L., Scalari, G., Hoyler, N., Giovannini, M. and Faist, J. InGaAs-AlInAs/InP terahertz quantum cascade laser. *Applied Physics Letters*, 2005. 87: 1–3.

56. Deutsch, C., Benz, A., Detz, H., Klang, P., Nobile, M., Andrews, A. M., Schrenk, W., Kubis, T., Vogl, P., Strasser, G. and Unterrainer, K. Terahertz quantum cascade lasers based on type II InGaAs/GaAsSb/InP. *Applied Physics Letters*, 2010. 97.

57. Dupont, E., Fathololoumi, S. and Liu, H. C. Simplified density-matrix model applied to three-well terahertz quantum cascade lasers. *Physical Review B - Condensed Matter and Materials Physics*, 2010. 81.

58. Jirauschek, C. and Kubis, T. Modeling techniques for quantum cascade lasers. *Applied Physics Reviews*, 2014. 1: 011307.

59. Kohen, S., Williams, B. S. and Hu, Q. Electromagnetic modeling of terahertz quantum cascade laser waveguides and resonators. *Journal of Applied Physics*, 2005. 97(5): 053106.

60. Strauch, D. and Dorner, B. Phonon dispersion in GaAs. *Journal of Physics: Condensed Matter*, 1990. 2(6): 1457–1474.

61. Donovan, K., Harrison, P. and Kelsall, R. W. Self-consistent solutions to the intersubband rate equations in quantum cascade lasers: Analysis of a $GaAs/Al_xGa_{1-x}As$ device. *Journal of Applied Physics*, 2001. 89: 3084–3090.

62. Indjin, D., Harrison, P., Kelsall, R. W. and Ikonić, Z. Self-consistent scattering theory of transport and output characteristics of quantum cascade lasers. *Journal of Applied Physics*, 2002. 91: 9019.

63. Indjin, D., Harrison, P., Kelsall, R. W. and Ikonić, Z. Influence of leakage current on temperature performance of GaAs/AlGaAs quantum cascade lasers. *Applied Physics Letters*, 2002. 81: 400–402.

64. Indjin, D., Harrison, P., Kelsall, R. W. and Ikonić, Z. Mechanisms of temperature performance degradation in terahertz quantum-cascade lasers. *Applied Physics Letters*, 2003. 82: 1347–1349.

65. Indjin, D., Ikonić, Z., Jovanović, V. D., Harrison, P. and Kelsall, R. W. Mechanisms of carrier transport and temperature performance evaluation in

terahertz quantum cascade lasers. *Semiconductor Science and Technology*, 2004. 19: S104–S106.

66. Chen, G., Yang, T., Peng, C. and Martini, R. Self-consistent approach for quantum cascade laser characteristic simulation. *IEEE Journal of Quantum Electronics*, 2011. 47: 1086–1093.

67. Saha, S. and Kumar, J. Complete rate equation modelling of quantum cascade lasers for the analysis of temperature effects. *Infrared Physics and Technology*, 2016. 79: 85–90.

68. Sirtori, C., Kruck, P., Barbieri, S., Collot, P., Nagle, J., Beck, M., Faist, J. and Oesterle, U. GaAs/AlxGa1-xAs quantum cascade lasers. *Applied Physics Letters*, 1998. 73: 3486–3488.

69. Iotti, R. C. and Rossi, F. Microscopic theory of hot-carrier relaxation in semiconductor-based quantum-cascade lasers. *Applied Physics Letters*, 2000. 76: 2265–2267.

70. Iotti, R. C. and Rossi, F. Carrier thermalization versus phonon-assisted relaxation in quantum-cascade lasers: A Monte Carlo approach. *Applied Physics Letters*, 2001. 78(19): 2902–2904.

71. Iotti, R. C. and Rossi, F. Nature of charge transport in quantum-cascade lasers. *Physical Review Letters*, 2001. 87: 146603.

72. Callebaut, H., Kumar, S., Williams, B. S., Hu, Q. and Reno, J. L. Importance of electron-impurity scattering for electron transport in terahertz quantum-cascade lasers. *Applied Physics Letters*, 2004. 84: 645–647.

73. Rochat, M., Faist, J., Beck, M., Oesterle, U. and Ilegems, M. Far-infrared (λ=88μm) electroluminescence in a quantum cascade structure. *Applied Physics Letters*, 1998. 73: 3724–3726.

74. Köhler, R., Iotti, R. C., Tredicucci, A. and Rossi, F. Design and simulation of terahertz quantum cascade lasers. *Applied Physics Letters*, 2001. 79(24): 3920–3922.

75. Tredicucci, A., Capasso, F., Gmachl, C., Sivco, D. L., Hutchinson, A. L. and Cho, A. Y. High performance interminiband quantum cascade lasers with graded superlattices. *Applied Physics Letters*, 1998. 73: 2101–2103.

76. Wanke, M. C., Capasso, F., Gmachl, C., Tredicucci, A., Sivco, D. L., Hutchinson, A. L. and Cho, A. Y. Quantum cascade lasers with double-quantum-well superlattices. *IEEE Photonics Technology Letters*, 2001. 13: 278–280.

77. Williams, B. S., Callebaut, H., Kumar, S., Hu, Q. and Reno, J. L. 3.4-THz quantum cascade laser based on longitudinal-optical-phonon scattering for depopulation. *Applied Physics Letters*, 2003. 82(7): 1015–1017.

78. Callebaut, H., Kumar, S., Williams, B. S., Hu, Q. and Reno, J. L. Analysis of transport properties of tetrahertz quantum cascade lasers. *Applied Physics Letters*, 2003. 83: 207–209.

79. Bonno, O., Thobel, J.-L. and Dessenne, F. Modeling of electron-electron scattering in Monte Carlo simulation of quantum cascade lasers. *Journal of Applied Physics*, 2005. 97(4): 043702.

80. Bonno, O., Thobel, J.-L. and Dessenne, F. Monte Carlo simulation of terahertz quantum cascade lasers: The influence of the modelling of carrier-carrier scattering. *Journal of Computational Electronics*, 2006. 5: 103–107.

81. Williams, B. S., Kumar, S., Callebaut, H., Hu, Q. and Reno, J. L. Terahertz quantum-cascade laser operating up to 137 K. *Applied Physics Letters*, 2003. 83: 5142–5144.

82. Jirauschek, C. Accuracy of transfer matrix approaches for solving the effective mass schrödinger equation. *IEEE Journal of Quantum Electronics*, 2009. 45: 1059–1067.

83. Jirauschek, C. and Lugli, P. Monte-Carlo-based spectral gain analysis for terahertz quantum cascade lasers. *Journal of Applied Physics*, 2009. 105(12): 123102.

84. Jirauschek, C., Matyas, A. and Lugli, P. Modeling bound-to-continuum terahertz quantum cascade lasers: The role of Coulomb interactions. *Journal of Applied Physics*, 2010. 107: 013104.

85. Jirauschek, C., Scarpa, G., Lugli, P., Vitiello, M. S. and Scamarcio, G. Comparative analysis of resonant phonon THz quantum cascade lasers. *Journal of Applied Physics*, 2007. 101: 086109.

86. Vitiello, M. S., Scamarcio, G., Spagnolo, V., Williams, B. S., Kumar, S., Hu, Q. and Reno, J. L. Measurement of subband electronic temperatures and population inversion in THz quantum-cascade lasers. *Applied Physics Letters*, 2005. 86: 111115.

87. Jirauschek, C. and Lugli, P. Limiting factors for high temperature operation of THz quantum cascade lasers. *Physica Status Solidi (C) Current Topics in Solid State Physics*, 2008. 5: 221–224.

88. Jirauschek, C. and Lugli, P. MC simulation of double-resonant-phonon depopulation THz QCLs for high operating temperatures. *Journal of Computational Electronics*, 2008. 7: 436–439.

89. Li, H., Cao, J. C., Tan, Z. Y., Han, Y. J., Guo, X. G., Feng, S. L., Luo, H., Laframboise, S. R. and Liu, H. C. Temperature performance of terahertz quantum-cascade lasers: Experiment versus simulation. *Journal of Physics D: Applied Physics*, 2009. 42: 025101.

90. Mátyás, A., Belkin, M. A., Lugli, P. and Jirauschek, C. Temperature performance analysis of terahertz quantum cascade lasers: Vertical versus diagonal designs. *Applied Physics Letters*, 2010. 96: 201110.

91. Matyas, A., Chashmahcharagh, R., Kovacs, I., Lugli, P., Vijayraghavan, K., Belkin, M. A. and Jirauschek, C. Improved terahertz quantum cascade laser with variable height barriers. *Journal of Applied Physics*, 2012. 111: 103106.

92. Han, Y. J. and Cao, J. C. Monte Carlo simulation of carrier dynamics in terahertz quantum cascade lasers. *Journal of Applied Physics*, 2010. 108: 093111.

93. Han, Y. J. and Cao, J. C. Temperature dependence of electron transport on a bound-to-continuum terahertz quantum cascade laser. *Semiconductor Science and Technology*, 2012. 27: 015002.

94. Jiang, A., Matyas, A., Vijayraghavan, K., Jirauschek, C., Wasilewski, Z. R. and Belkin, M. A. Experimental investigation of terahertz quantum cascade laser with variable barrier heights. *Journal of Applied Physics*, 2014. 115: 163103.

95. Shi, Y. B., Aksamija, Z. and Knezevic, I. Self-consistent thermal simulation of GaAs/Al 0.45Ga 0.55As quantum cascade lasers. *Journal of Computational Electronics*, 2012. 11: 144–151.

96. Bellotti, E., Driscoll, K., Moustakas, T. D. and Paiella, R. Monte Carlo study of GaN versus GaAs terahertz quantum cascade structures. *Applied Physics Letters*, 2008. 92(10): 101112.

97. Bellotti, E., Driscoll, K., Moustakas, T. D. and Paiella, R. Monte Carlo simulation of terahertz quantum cascade laser structures based on wide-bandgap semiconductors. *Journal of Applied Physics*, 2009. 105: 113103.

98. Bellotti, E. and Paiella, R. Numerical simulation of ZnO-based terahertz quantum cascade lasers. *Journal of Electronic Materials*, 2010. 39: 1097–1103.

99. Wacker, A. Gain in quantum cascade lasers and superlattices: A quantum transport theory. *Physical Review B - Condensed Matter and Materials Physics*, 2002. 66: 085326.

100. Wacker, A., Lindskog, M. and Winge, D. O. Nonequilibrium Green's function model for simulation of quantum cascade laser devices under operating conditions. *IEEE Journal on Selected Topics in Quantum Electronics*, 2013. 19: 1200611.

101. Lee, S. C. and Wacker, A. Nonequilibrium Green's function theory for transport and gain properties of quantum cascade structures. *Physical Review B - Condensed Matter and Materials Physics*, 2002.

102. Lee, S.-C., Banit, F., Woerner, M. and Wacker, A. Quantum mechanical wavepacket transport in quantum cascade laser structures. *Phys. Rev. B*, 2006. 73: 245320.

103. Banit, F., Lee, S.-C., Knorr, A. and Wacker, A. Self-consistent theory of the gain linewidth for quantum-cascade lasers. *Applied Physics Letters*, 2005. 86(4): 041108.

104. Kubis, T., Yeh, C., Vogl, P., Benz, A., Fasching, G. and Deutsch, C. Theory of nonequilibrium quantum transport and energy dissipation in terahertz

quantum cascade lasers. *Physical Review B - Condensed Matter and Materials Physics*, 2009. 79: 195323.

105. Schmielau, T. and Pereira, M. F. Nonequilibrium many body theory for quantum transport in terahertz quantum cascade lasers. *Applied Physics Letters*, 2009. 95: 231111.

106. Haldaś, G., Kolek, A. and Tralle, I. Modeling of mid-infrared quantum cascade laser by means of nonequilibrium Green's functions. *IEEE Journal of Quantum Electronics*, 2011. 47: 878–885.

107. Haldaś, G., Kolek, A., Pierścińska, D., Gutowski, P., Pierściński, K., Karbownik, P. and Bugajski, M. Numerical simulation of GaAs-based mid-infrared one-phonon resonance quantum cascade laser. *Optical and Quantum Electronics*, 2017. 49: 22.

108. Mátyás, A., Kubis, T., Lugli, P. and Jirauschek, C. Carrier transport in THz quantum cascade lasers: Are Green's functions necessary? *Journal of Physics: Conference Series*, 2009. 193: 012026. ISSN 17426596.

109. Mátyás, A., Kubis, T., Lugli, P. and Jirauschek, C. Comparison between semiclassical and full quantum transport analysis of THz quantum cascade lasers. *Physica E: Low-Dimensional Systems and Nanostructures*, 2010. 42: 2628–2631.

110. Willenberg, H., Döhler, G. H. and Faist, J. Intersubband gain in a Bloch oscillator and quantum cascade laser. *Physical Review B - Condensed Matter and Materials Physics*, 2003. 67: 085315.

111. Kumar, S. and Hu, Q. Coherence of resonant-tunneling transport in terahertz quantum-cascade lasers. *Physical Review B - Condensed Matter and Materials Physics*, 2009. 80: 0910.2959.

112. Weber, C., Wacker, A. and Knorr, A. Density-matrix theory of the optical dynamics and transport in quantum cascade structures: The role of coherence. *Physical Review B - Condensed Matter and Materials Physics*, 2009. 79: 165322.

113. Terazzi, R. and Faist, J. A density matrix model of transport and radiation in quantum cascade lasers. *New Journal of Physics*, 2010. 12: 033045.

114. Lindskog, M., Wolf, J. M., Trinite, V., Liverini, V., Faist, J., Maisons, G., Carras, M., Aidam, R., Ostendorf, R. and Wacker, A. Comparative analysis of quantum cascade laser modeling based on density matrices and non-equilibrium Green's functions. *Applied Physics Letters*, 2014. 105: 103106.

115. Iotti, R. C. and Rossi, F. Microscopic modelling of semiconductor-based quantum devices: A predictive simulation strategy. *Physica Status Solidi (B) Basic Research*, 2003. 238(3): 462–469.

116. Iotti, R. C. and Rossi, F. Microscopic theory of semiconductor-based optoelectronic devices. *Reports on Progress in Physics*, 2005. 68: 2533–2571.

117. Li, H., Cao, J. C. and Lü, J. T. Monte Carlo simulation of carrier transport and output characteristics of terahertz quantum cascade lasers. *Journal of Applied Physics*, 2008. 103: 103113.

118. Li, H., Cao, J. C., Han, Y. J., Guo, X. G., Tan, Z. Y., Lü, J. T., Luo, H., Laframboise, S. R. and Liu, H. C. A study of terahertz quantum cascade lasers: Experiment versus simulation. *Journal of Applied Physics*, 2008. 104: 043101.

119. Li, H., Cao, J. C., Tan, Z. Y. and Feng, S. L. Comparison of resonant-phonon-assisted terahertz quantum-cascade lasers with one-well injector and three-well module. *Journal of Applied Physics*, 2008. 104: 103101.

120. Li, H., Cao, J. C. and Liu, H. C. Effects of design parameters on the performance of terahertz quantum-cascade lasers. *Semiconductor Science and Technology*, 2008. 23: 125040.

121. Li, H., Cao, J. C., Luo, H., Laframboise, S. R., Wasilewski, Z. R. and Liu, H. C. The effect of phonon extraction level separation on the performance of three-well resonant-phonon terahertz quantum-cascade lasers. *Semiconductor Science and Technology*, 2009. 24: 065012.

122. Li, H. and Cao, J. C. Effect of injection coupling strength on terahertz quantum-cascade lasers. *Semiconductor Science and Technology*, 2011. 26: 095029.

123. Cao, J. C., Lü, J. T. and Li, H. Temperature performance of resonant-phonon-assisted terahertz quantum-cascade lasers. *Physica E: Low-Dimensional Systems and Nanostructures*, 2008. 41: 282–284.

124. Lee, S.-C., Giehler, M., Hey, R., Ohtsuka, T., Wacker, A. and Grahn, H. T. Dependence of lasing properties of GaAs/Al_xGa_{1-x}As quantum cascade lasers on injector doping density: theory and experiment. *Semiconductor Science and Technology*, 2004. 19: S45–S47.

125. Bellotti, E., Driscoll, K., Moustakas, T. D. and Paiella, R. Monte Carlo study of the temperature dependent performance of GaN versus GaAs terahertz quantum cascade structures. *Conference Proceedings - Lasers and Electro-Optics Society Annual Meeting-LEOS*, 2008: 266–267.

126. Li, H., Cao, J. C., LuÌĹ, J. T. and Han, Y. J. Monte Carlo simulation of extraction barrier width effects on terahertz quantum cascade lasers. *Applied Physics Letters*, 2008. 92(22): 221105.

127. Jirauschek, C. Monte Carlo study of carrier-light coupling in terahertz quantum cascade lasers. *Applied Physics Letters*, 2010. 96.

128. Jirauschek, C. Monte Carlo study of intrinsic linewidths in terahertz quantum cascade lasers. *Optics express*, 2010. 18: 25922–25927.

129. Jirauschek, C., Matyas, A., Lugli, P. and Amann, M.-C. Monte Carlo study of terahertz difference frequency generation in quantum cascade lasers. *Opt. Express*, 2013. 21: 6180–6185.

130. Iotti, R. C. and Rossi, F. Coupled carrier-phonon nonequilibrium dynamics in terahertz quantum cascade lasers: A Monte Carlo analysis. *New Journal of Physics*, 2013. 15.

131. Compagnone, F., Di Carlo, a. and Lugli, P. Monte Carlo simulation of electron dynamics in superlattice quantum cascade lasers. *Applied Physics Letters*, 2002. 80(6): 920.

132. Iotti, R. C., Ciancio, E. and Rossi, F. Quantum transport theory for semiconductor nanostructures: A density-matrix formulation. *Physical Review B - Condensed Matter and Materials Physics*, 2005. 72: 0509054.

133. RÃűsch, M., Beck, M., SÃijess, M. J., Bachmann, D., Unterrainer, K., Faist, J. and Scalari, G. Heterogeneous terahertz quantum cascade lasers exceeding 1.9 THz spectral bandwidth and featuring dual comb operation. *Nanophotonics*, 2018. 7(1): 237–242.

134. Garrasi, K., Mezzapesa, F. P., Salemi, L., Li, L., Consolino, L., Bartalini, S., De Natale, P., Davies, A. G., Linfield, E. H. and Vitiello, M. S. High Dynamic Range, Heterogeneous, Terahertz Quantum Cascade Lasers Featuring Thermally Tunable Frequency Comb Operation over a Broad Current Range. *ACS Photonics*, 2019. 6(1): 73–78.

135. Wienold, M., Schrottke, L., Giehler, M., Hey, R., Anders, W. and Grahn, H. Low-voltage terahertz quantum-cascade lasers based on LO-phonon-assisted interminiband transitions. *Electronics Letters*, 2009. 45: 1030–1031(1).

136. Li, L., Garrasi, K., Kundu, I., Han, Y., Salih, M., Vitiello, M., Davies, A. and Linfield, E. Broadband heterogeneous terahertz frequency quantum cascade laser. *Electronics Letters*, 2018. 54(21): 1229–1231.

137. Williams, B. S. *Terahertz Quantum Cascade Lasers*. Ph.D. Thesis. Massachusetts Institute Of Technology. 2003.

138. Loehr, J. P. and Manaresh, M. O. *Semiconductor quantum wells and superlattices for long-wavelength infrared detectors*. Artech house materials science library ed. Boston: Artech. 1993.

139. Nelson, D., Miller, R. and Kleinman, D. Band nonparabolicity effects in semiconductor quantum wells. *Physical Review B*, 1987. 35: 7770–7773.

140. Leavitt, R. P. Empirical two-band model for quantum wells and superlattices in an electric field. *Physical Review B*, 1991. 44: 11270–11280.

141. Bastard, G. *Wave mechanics applied to semiconductor heterostructures*. Paris: Jouve. 1988.

142. Burt, M. G. On the validity and range of applicability of the particle in a box model. *Applied Physics Letters*, 1994. 65(6): 717.

143. Zettili, N. *Quantum Mechanics: Concepts and Applications, 2nd edn.* vol. 52. 2009.

144. Harrison, P. *Quantum Wells, Wires and Dots*. Wiley, Chichester. 1999.

145. Goodnick, S. M. and Lugli, P. Effect of electron-electron scattering on nonequilibrium transport in quantum-well systems. *Physical Review B*, 1988. 37(5): 2578–2588.

146. Ando, T., Fowler, A. B. and Stern, F. Electronic properties of two-dimensional systems. *Reviews of Modern Physics*, 1982. 54(2): 437–672.

147. Cohen-Tannoudji, C., Diu, B. and Laloe, F. *Quantum Mechanics - Vol 2 - Cohen-Tannoudji*. 2006.

148. Martl, M., Darmo, J., Deutsch, C., Brandstetter, M., Andrews, A. M., Klang, P., Strasser, G. and Unterrainer, K. Gain and losses in THz quantum cascade laser with metal-metal waveguide. *Optics express*, 2011. 19: 733–738.

149. Nelander, R. and Wacker, A. Temperature dependence of the gain profile for terahertz quantum cascade lasers. *Applied Physics Letters*, 2008. 92.

150. Jukam, N., Dhillon, S. S., Oustinov, D., Zhao, Z.-Y., Hameau, S., Tignon, J., Barbieri, S., Vasanelli, a., Filloux, P., Sirtori, C. and Marcadet, X. Investigation of spectral gain narrowing in quantum cascade lasers using terahertz time domain spectroscopy. *Applied Physics Letters*, 2008. 93(10): 101115.

151. Jukam, N., Dhillon, S., Zhao, Z. Y., Duerr, G., Armijo, J., Sirmons, N., Hameau, S., Barbieri, S., Filloux, P., Sirtori, C., Marcadet, X. and Tignon, J. Gain measurements of THz quantum cascade lasers using THz time-domain spectroscopy. *IEEE Journal on Selected Topics in Quantum Electronics*, 2008. 14: 436–442.

152. Jukam, N., Dhillon, S., Oustinov, D., Zhao, Z. Y., Hameau, S., Barbieri, S., Filloux, P., Marcadet, X., Sirtori, C. and Tignon, J. Investigation into spectral gain narrowing in THz quantum cascade lasers above laser threshold using THz-time domain spectroscopy. *AIP Conference Proceedings*. 2009, vol. 1199. 473–474.

153. Jukam, N., Rungsawang, R., Dhillon, S. S., Oustinov, D., Madéo, J., Barbieri, S., Manquest, C., Sirtori, C., Khanna, S. P., Linfield, E., Davies, A. G. and Tignon, J. Terahertz amplifier based on gain switching in a quantum cascade laser. *AIP Conference Proceedings*. 2011, vol. 1399. 985–986.

154. Callebaut, H. and Hu, Q. Importance of coherence for electron transport in terahertz quantum cascade lasers. *Journal of Applied Physics*, 2005. 98(10): 104505.

155. Yariv, A. and Yeh, P. *Photonics*. Oxford University Press. 2006.

156. Fox, M. *Optical Properties of Solids*. Oxford University Press. 2001.

157. Poth, H., Bruch, H., Heyen, M. and Balk, P. Electron mobility in vapor-grown GaAs films. *Journal of Applied Physics*, 1978. 49(1): 285.

158. Huggard, P. G., Cluff, J. a., Moore, G. P., Shaw, C. J., Andrews, S. R., Keiding, S. R., Linfield, E. H. and Ritchie, D. a. Drude conductivity of highly doped GaAs at terahertz frequencies. *Journal of Applied Physics*, 2000. 87(5): 2382.

159. Katzenellenbogen, N. and Grischkowsky, D. Electrical characterization to 4 THz of N- and P-type GaAs using THz time-domain spectroscopy. *Applied Physics Letters*, 1992. 61: 840–842.

160. Walther, C., Scalari, G., Faist, J., Beere, H. and Ritchie, D. Low frequency terahertz quantum cascade laser operating from 1.6âĂĆtoâĂĆ1.8âĂĆTHz. *Applied Physics Letters*, 2006. 89(23): 231121.

161. Unterrainer, K., Colombelli, R., Gmachl, C., Capasso, F., Hwang, H. Y., Sergent, A. M., Sivco, D. L. and Cho, A. Y. Quantum cascade lasers with double metal-semiconductor waveguide resonators. *Applied Physics Letters*, 2002. 80(17): 3060–3062.

162. Hoffman, A. J., Alekseyev, L., Howard, S. S., Franz, K. J., Wasserman, D., Podolskiy, V. A., Narimanov, E. E., Sivco, D. L. and Gmachl, C. Negative refraction in semiconductor metamaterials. *Nature materials*, 2007. 6: 946–950.

163. Kogelnik, H. and Shank, C. V. Coupled-wave theory of distributed feedback lasers. *Journal of Applied Physics*, 1972. 43(5): 2327–2335.

164. Courant, R. Variational Methods for the Solution of Problems of Equilibrium and Vibrations. *Bull. Amer. Math. Soc.*, 1943. 49: 1 – 23.

165. Jin, J.-M. *The Finite Element Method in Electromagnetics*. third edition ed. New Jersey: John Wiley and Sons. 2014.

166. Huebner, K. H., Dewhirst, D. L., Smith, D. E. and Byrom, T. G. *The Finite Element Method for Engineers*. fourth edition ed. New York: John Wiley and Sons. 2001.

167. Sadiku, M. N. . *Numerical Techniques in Electromagnetics*. second edition ed. Boca Raton, FL: CRC Press. 2001.

168. Strang, G. and Fix, G. J. *An Analysis of the Finite Element Method*. Prentice-hall series in automatic computation ed. Englewood Cliffs, NJ: Prentice Hall. 1973.

169. Pelosi, G., Coccioli, R. and Selleri, S. *Quick Finite Elements For Electromagnetic Waves*. second edition ed. Norwood, MA: Artech House. 2009.

170. Rao, N. N. *Elements of Engineering Electromagnetics*. fifth edition ed. Upper Saddle River, New Jersey: Prentice Hall. 2000.

171. Shewchuk, J. R. Delaunay refinement algorithms for triangular mesh generation. *Computational Geometry*, 2002. 22(1): 21–74. 16th ACM Symposium on Computational Geometry.

172. Shewchuk, J. R. *Delaunay Refinement Algorithms for Triangular Mesh Generation*. Ph.D. Thesis. Department of Electrical Engineering and Computer Science, University of California at Berkeley. 2001.

173. Andonegui, I. and Garcia-Adeva, A. J. The finite element method applied to the study of two-dimensional photonic crystals and resonant cavities. *Optics express*, 2013. 21: 4072–92.

174. Faist, J. *Quantum Cascade Lasers*. Oxford University Press. 2013.

175. Michaelson, H. B. The work function of the elements and its periodicity. *Journal of Applied Physics*, 1977. 48(11): 4729–4733.

176. Davis, T. A. and Duff, I. S. An Unsymmetric-Pattern Multifrontal Method for Sparse LU Factorization. *SIAM Journal on Matrix Analysis and Applications*, 1997. 18: 140–158.

177. Sachs, R. and Roskos, H. Mode calculations for a terahertz quantum cascade laser. *Optics express*, 2004. 12: 2062–2069.

LIST OF PUBLICATIONS

Indexed Journal (SCOPUS)

1. Mohd Asmu'i Mohd Akil, Khalid Akabli, Amiruddin Shaari, Mohd Khalid Kasmin, Zulkafli Othaman, The Study Of Optical Gain For Terahertz Quantum Cascade Laser Using Density Matrix Method, *Jurnal Teknologi Malaysia*, 78:9 (2016) 123-128. eISSN 2180-3722

Indexed conference proceedings

1. M. Asmu'i M. Akil, Amiruddin Shaari, M. Khalid Kasmin, Zulkafli Othaman, Study Of Resonant Phonon THz Quantum Cascade Laser Design Using Density Matrix Method, *Proceeding of 2nd International Science Postgraduate Conference 2014 (ISPC 2014)*, March 10-12, 2014, Fakulti Sains, Universiti Teknologi Malaysia, pp 176-185.

Non-Indexed conference proceedings

1. M. Asmu'i M. Akil, Khalid Akabli, Amiruddin Shaari, M. Khalid Kasmin, Zulkafli Othaman, The Gain of THz Quantum Cascade Laser Using Density Matrix Method for Resonant Phonon Design, Presentation at the *28^{th} Regional Conference on Solid State Science and Technology*, Copthorne Hotel, Cameron Highlands, Pahang, 25 - 27 November 2014.
2. M. Asmu'i M. Akil, Amiruddin Shaari, M. Khalid Kasmin, Zulkafli Othaman, THz Quantum Cascade Laser Design for Resonant Phonon and Bound-To-Continuum Using Density Matrix, Presentation at the *Nano Scitech 2014 & IC-net 2014*, Institute of Leadership and Quality Management (iLQAM), Universiti Teknologi Mara, Shah Alam, Selangor, 28 February - 3 March 2014.